Journal Pre-proofs

Thermal performance of water driven flow of nanoparticle's shape due to double sided forced convection enclosed in a porous corrugated duct

Anh Tuan Hoang, Syed Saqib Shah, Rizwan Ul Haq, Tri Hieu Le, Luthais B. McCash

Please cite this article as: A. Tuan Hoang, S. Saqib Shah, R. Ul Haq, T. Hieu Le, L.B. McCash, Thermal performance of water driven flow of nanoparticle's shape due to double sided forced convection enclosed in a porous corrugated duct, *Journal of Molecular Liquids* (2021), doi: https://doi.org/10.1016/j.molliq.2021.118046

Thermal performance of water driven flow of nanoparticle's shape due to double sided forced convection enclosed in a porous corrugated duct

Anh Tuan Hoang[1], Syed Saqib Shah[2], Rizwan Ul Haq[3,*], Tri Hieu Le[4,*], Luthais B. McCash[5]

[1]*Institute of Engineering, Ho Chi Minh city University of Technology (HUTECH), Ho Chi Minh city, Vietnam*

[2]*Department of Computer Science, Bahria University Islamabad Campus, Sector E-8, 44000 Islamabad, Pakistan.*

[3]*Department of Electrical Engineering, Bahria University Islamabad Campus, Sector E-8, 44000 Islamabad, Pakistan.*

[4]*PATET Research Group, Ho Chi Minh city University of Transport, Ho Chi Minh city, Vietnam*

[5]*Department of Mathematics, College of Science and Engineering University of Leicester, University Road, Leicester, LE1 7RH, UK*

Abstract

In this article, a complex nature structure is simulated by introducing the nanofluid that contains various shape of nanoparticles through forced convection and thermal diffusion. Double sided lid-driven in a porous curved cavity is dealt to handle the forced convection phenomenon. Additionally, effect of internal heat generation/absorption is also considered. The horizontal and vertical walls are moving with a constant speed U_o and V_o, respectively, which are further divided into two moving lids. The flat and curved walls are kept at constant temperature T_H and T_C respectively. The governing equations are discretized and solved through Glariken residual method by mean of Finite Element Method (FEM). The effect of various directional velocity, porous medium (Da), Reynold's number (Re), internal heat generation/ absorption coefficient (Q) and solid concentration of nanoparticles (ϕ) are investigated on transfer rate of heat in the form of Nusselt number, isotherm, streamlines, temperature and velocity profile. Result reveals that heat

---

* Corresponding author: R. U. Haq (rizwanulhaq.buic@bahria.edu.pk)

Tri Hieu Le (hieu.le@ut.edu.vn)

is generated in cavity when the direction of velocity of moving wall is in the opposite inward direction. The heat transfer rate decreases in the case of internal heat generation and increases for nanoparticles.

Keywords: Forced convection; cavity; finite element method; double lid-driven; curve grove.

Nomenclature			
x^*, y^*	Cartesian coordinates (m)	**Greek symbols**	
u^*, v^*	Velocities in x^* and y^* directions m/s	α	thermal diffusivity (m^2/s)
Da	Darcy number	θ^*	Dimensionless temperature
Re	Reynolds number	β	Thermal expansion coefficient
Ri	Ricardson number	γ	Penalty parameter
Gr	Grashof number	ρ	density (kg/m^3)
Pr	Prandtl number	μ	dynamic viscosity $(kg/m/s)$
H	characteristic length	ν	kinematic viscosity (m^2/s)
g	Acceleration due to gravity	Ω	computational domain
Q	Heat generation/absorption coefficient	k	thermal conductivity
Nu	Nusselt number	**Subscripts**	
X^*, Y^*	dimensionless Cartesian coordinates	avg	average
U^*, V^*	dimensionless velocities	o	Reference state
T^*	Temperature	f	Base fluid
c	specific heat	nf	nanofluid

2

p	Dimensional pressure	c	cold surface
P	Dimensionless pressure	p	(nano) particle
m	Shape factor of nanoparticle		

1. Introduction

Thermal enhancement of the heat transfer is one of the major problems in engineering devices such as ventilation, heating, cooling devices, heat exchanger, and drying food. In industrial equipment, to enhance the heat flow nanofluid has a significant role in the recent decade. A high heat transfer rate is required for cooling processors and electronic devices. For this purpose, the nanofluid suspension is used which is formed from nanoparticle and base fluid. The applications of nanoparticles in industries have been studied recently in [1-5]. Various experimental and theoretical models have been introduced to estimate the thermophysical properties of nanofluids which are based on the size of nanoparticle, temperature, the shape of particle, and interaction of the nanoparticle and pure water.

Nowadays, the importance of heat transfer is significant especially in vehicles, avionics, textile, food, and petrochemical industries, etc. The transportation of fluid in a lid-driven cavity is important due to the forced convection. Haq et al. [6] studied the trapezoidal cavity which was partially heated, and they also discussed the convection of fluid flow. A numerical analysis done by Mansour and Ahmed [7] had conducted the numerical analysis on a lid-driven cavity with a bottom heat source. The effect of nanoparticles on heat transfer rate was studied by Boutra et al. [8]. Mixed convection in a lid-driven cavity was studied by Esfe et al. [9] withthe inside of the heated obstacle. Nanofluid mixed convection inside a sinusoidal (heated) lid-driven cavity was investigated by Abbasian Arani et al. [10]. Ghofrani et al. [11] analyzed the forced convection of heat transfer of ferrofluid flow in a circular copper tube in addition to the magnetic field. Nasrin et al. [12] investigated the mixed convection in a double lid-driven triangular wavy cavity, which is filled with CuO nanoparticles having different nanofluid viscosity models, namely the Pak and Cho [13] correlation and Brinkman [14] model. In a square cavity, the effect of nanofluid was reported by Ho et al. [15]. Izadi et al. [16] analysed the forced convection in the annulus. That

annulus filled with Al_2O_3 nanofluid concertation. In that case, they reported that friction coefficient is highly dependent on the nanofluid concentration. Mahmoodi [17] investigated the mixed convection of Al_2O_3 water nanofluid in a lid-driven enclosure having a bottom wall is hot and moving with constant velocity. In a rectangular cavity, the effect of nanofluid properties in a mixed convection case was reported by Mazrouei Sebdani et al. [18].

Porous media has a high impact on heat transfer in the cavity with the presence of nanoparticles. It enhances the transportation of heat in the enclosure. In literature, many researchers [19-30] have reported that high thermal conductivity is developed in the porous cavity due to the presence of nanofluid particles. Chatterjee et al. [31] worked in a lid-driven cavity containing the rotating cylinder and nanofluids. In that enclosure, combined convection was performed for heat transportation. The top wall moving with constant speed from left to right while all other walls are fixed or stationary. They also analysed the effect of rotating cylinder speed on heat transfer. Heat and mass transfer were reviewed by Yazid et al. [32] with the presence of CNT-nanoparticle characteristics. Alsabery et al. [33] investigated the effect of nanofluid particles in the trapezoidal cavity with the non-uniform temperature of the sidewall. Chamkha [34] analysed the effect of internal heat generation coefficient and magnetic field on combined convection in a lid-driven cavity. The result shows that the Nusselt number decreases with the increase of the magnetic field. Oztop et al. [35] investigated the heat transfer and convection in MHD lid-driven cavity which has a heated corner. They reported that an inverse relation is developed between Hartmann number and heat transfer. For engineering, the higher impact of heat transfer in a porous cavity with the nanofluids was investigated by [36-50].

The main purpose of this study is to analyze the heat transfer and fluid flow with the forced convection of nanofluids through a porous two-dimensional double lid-driven curve groves cavity by using Finite Element Method (FEM). In the present article, the effect of heat generation/absorption coefficient on temperature and Nusselt number are investigated. The effect of different directional velocities of the moving walls on isotherm and streamline is analyzed. Graphical representations of the core parameter on heat flow, heat transfer, and velocity are shown in section 4.

2. Mathematical formulation

Consider the two-dimensional viscous flow enclosed by curve shape that is heated from the bottom and left wall, flow is due to the fully heated walls of lid-driven. In order to construct the

mathematical model inside the partially corrugated cavity (see Figure 1), we have defined various constraints which are mandatory to examine the theoretical investigation. For an incompressible fluid, a steady, two-dimensional Newtonian model is considered with a constant density. Based upon the constant density, the conservation equations are defined as:

Continuity equation:
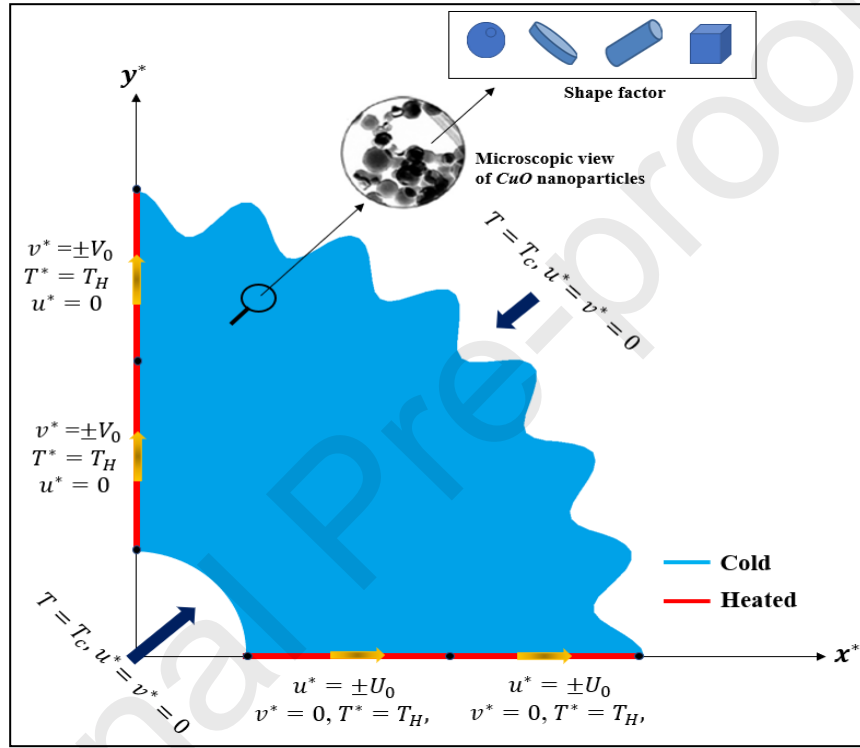
$$\nabla . \boldsymbol{v} = 0, \tag{1}$$

Fig. 1: Geometry of the lid-driven cavity.

Momentum equations in $x^* -$ and $y^* -$directions by [51]:

$$v^* \frac{\partial u^*}{\partial y^*} + u^* \frac{\partial u^*}{\partial x^*} = -\frac{1}{\rho_{nf}} \frac{\partial p}{\partial x^*} + \frac{\mu_{nf}}{\rho_{nf}} \left(\frac{\partial^2 u^*}{\partial y^{*2}} + \frac{\partial^2 u^*}{\partial x^{*2}} - \frac{u^*}{k} \right), \tag{2}$$

$$v^* \frac{\partial v^*}{\partial y^*} + u^* \frac{\partial v^*}{\partial x^*} = -\frac{1}{\rho_{nf}} \frac{\partial p}{\partial y^*} + \frac{\mu_{nf}}{\rho_{nf}} \left(\frac{\partial^2 v^*}{\partial y^{*2}} + \frac{\partial^2 v^*}{\partial x^{*2}} - \frac{v^*}{k} \right) + \frac{(\rho\beta)_{nf}}{\rho_{nf}} g(T^* - T_o), \tag{3}$$

Energy equation:

$$v^* \frac{\partial T^*}{\partial y^*} + u^* \frac{\partial T^*}{\partial x^*} = \alpha_{nf} \nabla^2 T^* + \frac{Q_o}{(\rho c_p)_{nf}} (T^* - T_o) \tag{4}$$

2.1 Physical problem

5

In the above equation, $\left(\frac{\partial}{\partial x^*}, \frac{\partial}{\partial y^*}, 0 \right)$ are the partial differential operator and $(u^*, v^*, 0)$ are velocity field according to the two-dimensional flow $(X^* -$ and $Y^* -$directions). Where T and T_c are the temperature of fluid and cold surface respectively. Moreover, P is the initial pressure exerted by a fluid particle in the $X^* -$ and $Y^* -$directions. In the above system of equations, μ_{nf}, ρ_{nf}, c_p and g are the dynamic viscosity, density, specific heat, and gravity respectively. Various techniques are used for the thermophysical properties of the solid volume fraction of nanofluid formulation. In this article, we used the previous technique, in which it depends only on the nanoparticles.

The effective density (ρ_{nf}) of the nanofluid is

$$\rho_{nf} = (1 - \phi)\rho_f + \phi\rho_p \tag{5}$$

ϕ (solid volume) fraction, ρ_f (fluid density) and ρ_p (solid fraction density) and the heat capacity of the fluid is given by

$$\left(\rho c_p\right)_{nf} = (1 - \phi)\left(\rho c_p\right)_f + \phi\left(\rho c_p\right)_p \tag{6}$$

The thermal expansion coefficient of the nano-fluid can be determined by the expression

$$(\rho\beta)_{nf} = (1 - \phi)(\rho\beta)_f + \phi(\rho\beta)_p \tag{7}$$

Here β_f and β_p represent the thermal expansion coefficient of the fluid and solid fractions respectively.

α_{nf} be the thermal diffusivity of the nanofluid is defined as:

$$\alpha_{nf} = \frac{k_{nf}}{\left(\rho c_p\right)_{nf}} \tag{8}$$

For spherical nanoparticles thermal conductivity (k_{nf}) of the nanofluid modelled by Maxwell [52]. Which is written in mathematical form as;

$$\frac{k_{nf}}{k_f} = \frac{k_p + (m-1)k_f - (m-1)\phi(k_f - k_p)}{k_p + (m-1)k_f + \phi(k_f - k_p)} \tag{9}$$

The dynamic viscosity of the nanofluid is written as;

$$\frac{\mu_{nf}}{\mu_f} = \frac{1}{(1-\phi)^{2.5}} \tag{10}$$

The dimensionless variables are introduced:

$$(X^*, Y^*) = \frac{(x^*, y^*)}{H}, (U^*, V^*) = \frac{(u^*, v^*)}{V_o}, \ P = \frac{p}{\rho_{nf} V_o^2}, \ \theta^* = \frac{T^* - T_H}{T_H - T_c}, \tag{11}$$

$$Ri = \frac{Gr}{Re^2}, \ Re = \frac{V_o H}{\nu_f}, \nu_{nf} = \frac{\mu_{nf}}{\rho_{nf}}, Q = \frac{Q_o H^2}{(\rho c_p)_f \alpha_f}, Pr = \frac{\nu_f}{\alpha_f}.$$

In the above expressions, Re is the Reynolds number, Ri is the Richardson number, Q is the heat generation/absorption parameter, and Pr is the Prandtl number. Using (5) into the system of equations (2)-(4), we get

Table 1
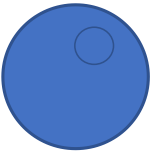
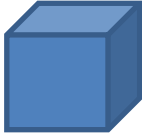Value of shape factor of nanoparticle and base fluid:

Spherical		$m = 3.3$
Platelet		$m = 5.7$
Cylindrical		$m = 4.8$
Brick		$m = 3.7$

Table 2

Thermo-physical properties of nanofluid particles and based fluid:

Physical properties	$C_p (J/kgK)$	$\rho(kg/m^3)$	$K(W/mK)$	$\beta \times 10^5 (1/K)$	$\sigma(\Omega.m)^{-1}$
Water	4179	997.1	0.613	21	0.05
CuO	540	6500	18	29	10^{-10}

7

$$\frac{\partial U^*}{\partial X^*} + \frac{\partial V^*}{\partial Y^*} = 0, \tag{12}$$

$$U^* \frac{\partial U^*}{\partial X^*} + V^* \frac{\partial U^*}{\partial Y^*} = -\frac{\partial P^*}{\partial X^*} + \frac{1}{Re}\left(\frac{\nu_{nf}}{\nu_f}\right)\left(\frac{\partial^2 U^*}{\partial X^{*2}} + \frac{\partial^2 U^*}{\partial Y^{*2}} - \frac{U^*}{Da}\right), \tag{13}$$

$$U^* \frac{\partial V^*}{\partial X^*} + V^* \frac{\partial V^*}{\partial Y^*} = -\frac{\partial P^*}{\partial Y^*} + \frac{1}{Re}\left(\frac{\nu_{nf}}{\nu_f}\right)\left(\frac{\partial^2 V^*}{\partial X^{*2}} + \frac{\partial^2 V^*}{\partial Y^{*2}} - \frac{V^*}{Da}\right) + Ri\,\frac{(\rho\beta)_{nf}}{\rho_{nf}\beta_f}\theta^*, \tag{14}$$

$$U^* \frac{\partial \theta^*}{\partial X^*} + V^* \frac{\partial \theta^*}{\partial Y^*} = \left(\frac{\alpha_{nf}}{\alpha_f}\right)\frac{1}{PrRe}\left(\frac{\partial^2 \theta^*}{\partial X^{*2}} + \frac{\partial^2 \theta^*}{\partial Y^{*2}}\right) + \left(\frac{Q}{Pr\,Re}\right)\frac{(\rho c_p)_f}{(\rho c_p)_{nf}}\theta^*. \tag{15}$$

2.2 Boundary conditions

The dimensionless form of the boundary conditions is:

a) At the bottom solid wall (Ω_1 & Ω_2):

$$U^* = 1; V^* = 0; \theta^* = 1, \qquad \text{when}$$
$$\Omega_1 = \{(X^*, Y^*)\epsilon R^2 \,/\, 0.27 \leq X^* \leq 0.365 \text{ and } Y^* = 0\},$$
$$\Omega_2 = \{(X^*, Y^*)\epsilon R^2 \,/\, 0.365 \leq X^* \leq 1 \text{ and } Y^* = 0\}, \tag{16}$$

b) At the left solid wall (Ω_3 & Ω_4):

$$U^* = 0; V^* = 1; \theta^* = 1, \qquad \text{when}$$
$$\Omega_3 = \{(X^*, Y^*)\epsilon R^2 \,/\, 0.27 \leq Y^* \leq 0.365 \text{ and } X^* = 0\}$$
$$\Omega_4 = \{(X^*, Y^*)\epsilon R^2 \,/\, 0.365 \leq Y^* \leq 1 \text{ and } X^* = 0\} \tag{17}$$

c) At solid corrugate wall (Ω_5):

$$U^* = 0, V^* = 0, \theta^* = 0, \tag{18}$$

d) At the curve surface:

$$U^* = 0, V^* = 0, \theta^* = 0, \text{ when } \Omega_5 = \{(X^*)^2 + (Y^*)^2 = (r_2)^2\}. \tag{19}$$

Where the center of the inner circle is $(0,0)$ and radius is 0.27.

3. Methodology and comparison

To solve the dimensionless equations (12)-(15) with their corresponding boundary conditions, we apply Finite Element Method. In that study, Galerkin weighted residual scheme has been applied to solve the dimensionless equations. This numerical method is well analyzed by [53-54]. The geometry of the problem is divided into sub-domain in the form of non-uniform triangular meshes. Where meshes are composed of triangular elements, which contain nodes. In this study, velocities and temperatures are related to these nodes and at the corners, the nodes are associated with pressure. The pressure is defined in the form of a lower-order polynomial which satisfies the

8

continuity equation. Galerkin weighted residual scheme in the form of shape function converted the momentum and energy equations of nanofluids into integral equations. The integral equation of each term is converted into non-linear algebraic equations by using Gauss quadrature method. To solve the nonlinear equation in the form of the matrix, Newton Raphson technique is implemented to solve the Partial differential equations.

The local Nusselt number in dimensionless form at horizontal and vertical lid walls are written in mathematical form as

$$Nu_{\Omega_1} = -\frac{k_{nf}}{k_f}\left(\frac{\partial\theta^*}{\partial Y^*}\right)_{Y^*=0} = Nu_{\Omega_2} \tag{20a}$$

$$Nu_{\Omega_3} = -\frac{k_{nf}}{k_f}\left(\frac{\partial\theta^*}{\partial X^*}\right)_{X^*=0} = Nu_{\Omega_4} \tag{20b}$$

In this section, we have validated the numerical result of the present problem with other manuscripts. Thermal performance in the lid-driven square model can be compared with earlier works done by Khanafer and Chamkha [55] and Iwatsu et al. [56] in Fig.2(a), our current thermal work in contour with limiting conditions is depicted in Fig. 2(b).

3.1 Mesh Independency

The various grid has resorted for each case. The average Nusselt number calculated for different grids at the wall is shown in Table 3.

Table 3

Comparison of Average Nusselt number for uniform and nonuniform mesh distribution at the wall, when $Re = 300, Da = 10^{-3}, Q = 5, \phi = 0.2, Pr = 6.2$.

Grid size	30×30	40×30	60×25	45×60	65×65
Avg. Nusselt	-1.64531	-1.65621	-1.66243	-1.66250	-1.66250

Table 4

Average Nusselt number when different shapes of nanoparticles, when $Re = 350, \ Q = 10, \phi = 0.1, Pr = 6.2$.

Da	Spherical	Bricks	Cylindrical	Platelet
10	-1.29828	-1.35907	-1.44892	-1.51773

Table 5

Comparison of the mean Nusselt number at the top wall, for different values of Re at $Pr = 0.71$,

Re	Iwatsu et al. [56]	Khanafer & Chamkha [55]	Present work
100	1.94	2.01	1.93
400	3.84	3.91	3.90
1000	6.33	6.33	6.33

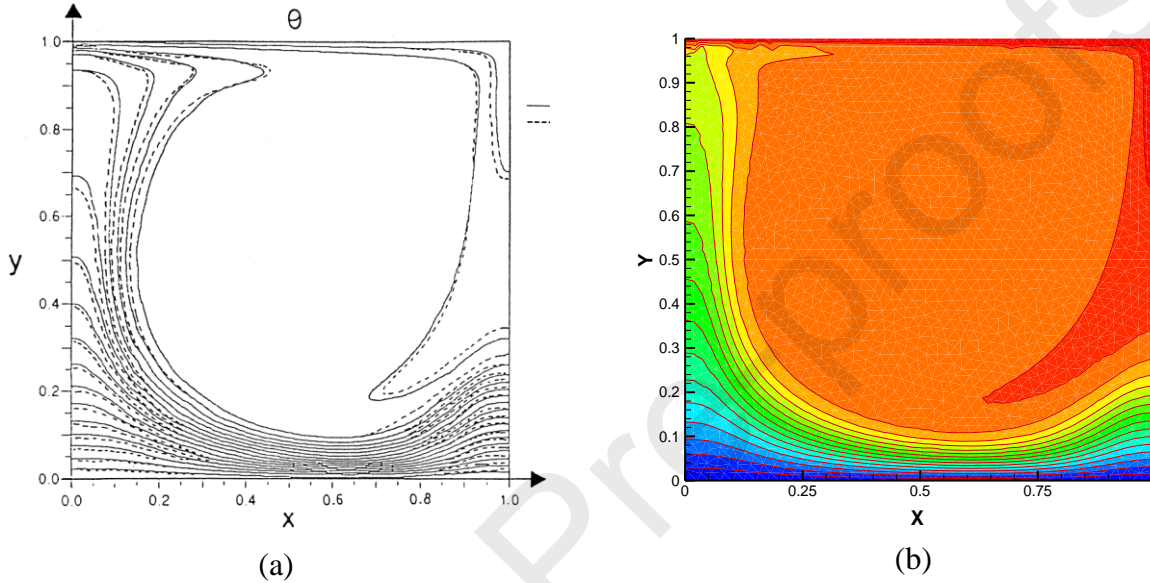(a)   (b)

Fig. 2: Comparison of isotherms in a square cavity: (a) Khanafer and Chamkha [55] (straight line) and Iwatsu et al. [56] (dotted line) when $Re = 10^3$ (b) Present work.

4. Results and Discussion

In this script, forced convection of water-based nanofluid in a corrigent porous cavity with a partially double lid-driven wall is investigated using Finite element method (FEM). Numerical results are illustrated for various values of Reynolds number ($Re = 100$ to 400), double lid wall with different uniform velocities, Darcy number ($Da = 0.0001$ to 10), Heat generation coefficient ($Q = -1000$ to 75), and the solid volume fraction of nanoparticles (CuO). Table 4 illustrates the shape of the nanoparticle effect on the average Nusselt number. In the case of spherical shape maximum values of Nusselt number are recorded. Simulation is performed for different parameters when the spherical shape of the nanoparticle is used.

4.1 Effect of the double moving lid-wall direction

Case I: **Horizontal lid moves left to right and vertical lid wall moves bottom to top.**

Fig. 3(a) represents the streamline due to the moving lid wall with a constant temperature. In the case of lid walls, symmetric lines are generated near the lid walls and heat is generated inside of the cavity. Fig. 3(b) illustrates the streamlines profile in that case. The molecular movement of the particle is quite similar around the lid walls. It creates two bigger eddies near the wall.

Case II: **Lid walls move with opposite inward directional velocity.**

Fig. 3(c) and (d) illustrate isotherm and streamlines profile respectively. The more heat is generated in that case and heat generated inside the enclosure is due to the inside movement of the two-lid moving wall. Heat generation is clearly seen in the mid of the lid walls. Fig. 3(d) illustrates the path of the molecule movement inside the enclosure. More eddies are created due to the opposite direction of lid-moving walls and counterclockwise rotation of the molecular movements. That eddy may be the formation of the secondary eddies due to the partition of the major eddies.

Case III: **Lid walls move with opposite outward directional velocity.**

From Fig. 3(e), it is observed that the isotherm spread near the wall, and a major part of the heat was located near the corrugated wall. The symmetric hope of the isotherm lines was created due to the opposite direction of the bottom vertical and left horizontal wall. Fig. 3(f) demonstrates streamlines in the shape of two larger and two smaller eddies near the wall.

Case IV: Horizontal walls move from right to left and vertical walls move from top to bottom.

Fig. 3(g) illustrates the effect of the inside movement of the lid walls on streamlines. It is observed that the heat distribution near the corrugated wall is maximum than the lid wall and isotherm lines are quite stable away from the lid walls. Through the molecular movement of the particles, two bigger eddies are created which cover the whole cavity in the form of lines.

Fig. 4(a)-(e) represents the temperature, velocity profile, and Nusselt number for different lid wall constraints. Fig. 4(a) illustrates that the maximum heat transfer is noticed because of the right horizontal and top vertical partial wall which move with the velocity $U_R = V_T = -1$. Inside the movement of the walls, more heat is created within the cavity. The minimum temperature gradient is recorded in the case of outside movement of all lid walls. Minimum temperature gradient recorded in case of outside movement of all lid walls. Fig. 4(b) and (c) illustrate the Nusselt number horizontal and vertical mean position. Nusselt number decreases in case of outside movement inside movement of the lid walls. But attain its maximum flow rate of heat when the velocity of the moving wall is $U_L = V_B = -1$. In that case, significant Nusselt number increases

in the middle of the cavity. Horizontal and vertical velocity profile, in this case, is demonstrated in Fig. 4(d) and (e). Its significant effect on velocity profile could be due to drag force variation near the moving walls.

4.2 Effect of the Reynolds Number

Fig. 5 (a-h) shows the impact of Reynolds number on streamlines and isotherms for nanofluid particles in a corrigent enclosure. As it can be noticed from isotherm plots that at low *Re* the contour is uniformly distributed with the heat on both sides of the lid walls.
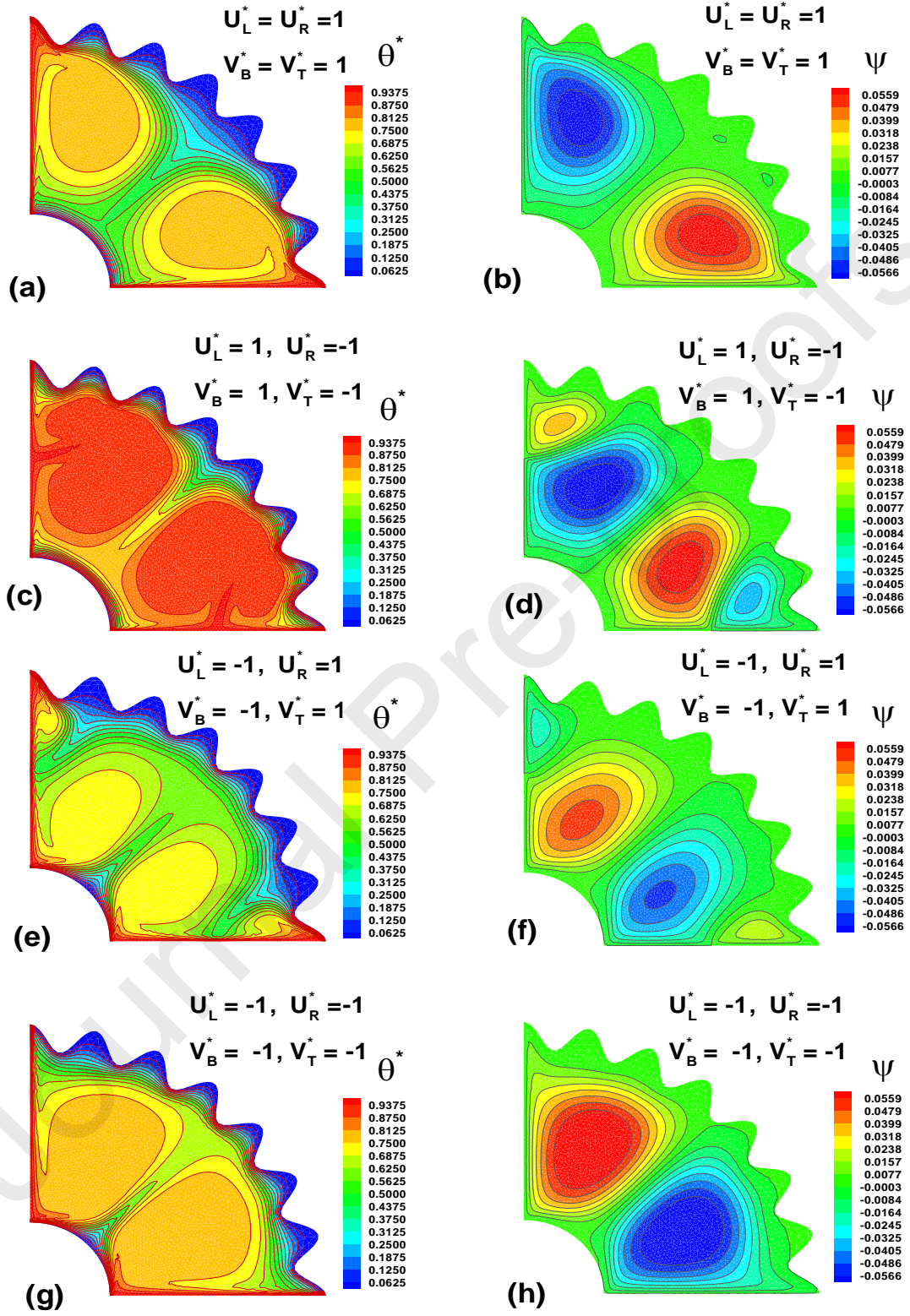
Fig. 3. Effect of various lid-moving walls on the isotherm and streamlines.
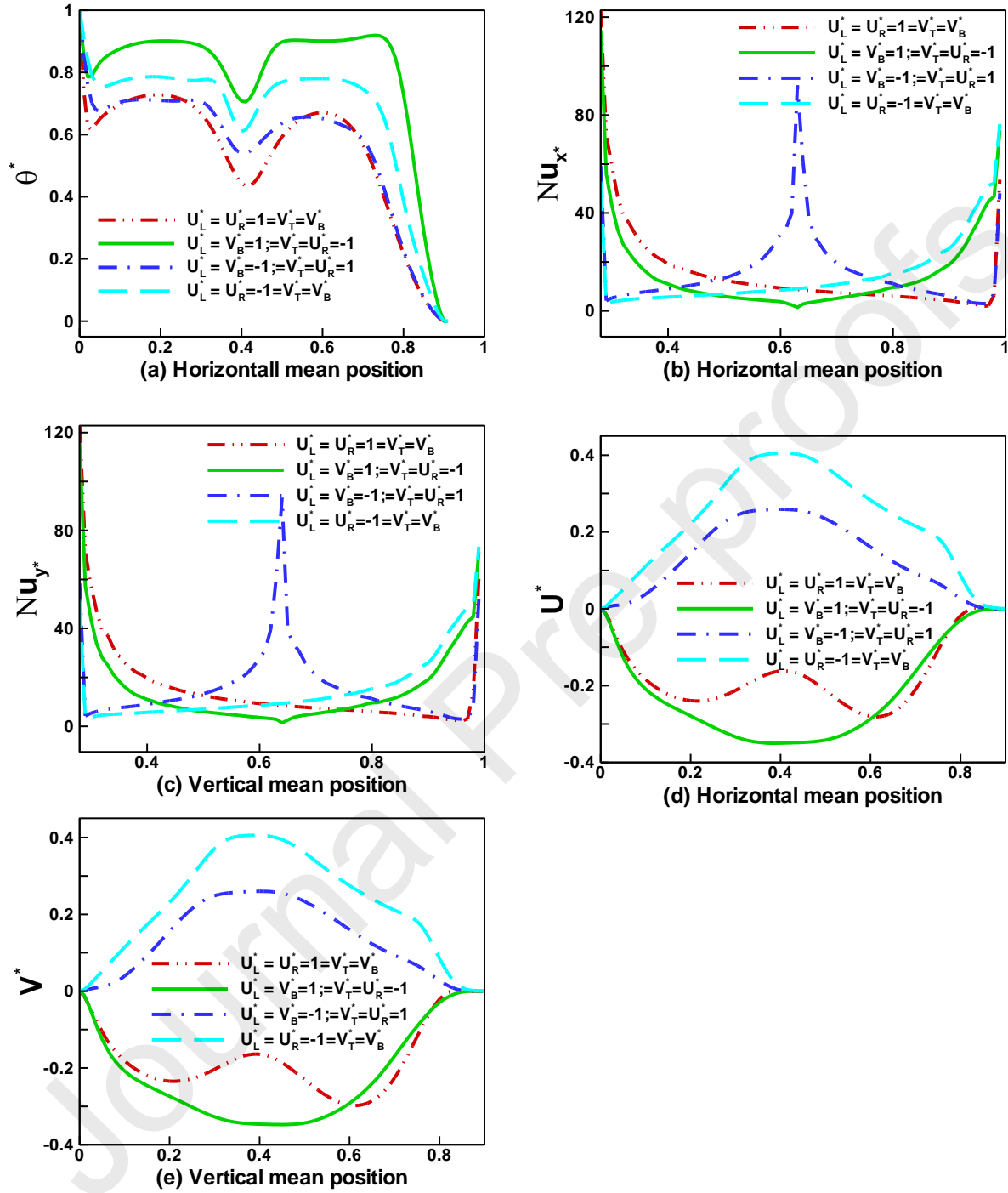
Fig. 4. Effect of various lid moving walls on the Temperature, velocity profile, and Nusselt number.

Isotherm lines create a circular format, and the isotherm lines are stronger as Re increases. The effect of forced convection is weaker for decreasing values of Re, the number of heated lines is reduced. However, as the Reynolds number rises, it steadily rises. For a maximum value of Re, the heat flux rises, making forced convection the dominating mode of transport. This indicates the dominant forced convection of heat in the cavity. Due to the lid moving at the middle of the lid walls the heat lines tilt towards the upward direction with the increase in Re. For low Reynold numbers, the flow pattern is symmetric and creates eddies around the moving walls. For the smaller value of Reynolds number small circular vertex rotation generates creates near the lid walls. With an increase in Re, vertex rotation size increases and remains quite stable for maximum value parameter. As with the increasing of Re, the symmetry of the flow is disturbed as shown in Fig 5(h).

Fig. 6 (a)-(e) presents the effect of Re on velocity, temperature, and Nusselt number in the lid cavity. Fig. 6 (a) illustrates that the temperature distribution increases inside the cavity with increasing of Re. For high Re, greater convection is produced inside the cavity. Heat flow increases due to the molecular movement of the particles. Nusselt number also varies due to the moving lid walls and increasing of Re. In the middle, strong convection is being observed. Horizontal and vertical velocity decreases with the increase in Re in the middle of the cavity. However, increases in the end of the cavity could be due to the moving walls with constant velocities.

4.3 Effect of the Porous Medium

Fig. 7 (a)-(h) presents the effect of Darcy number on isotherm and streamline profile for the maximum value of Reynolds number. The heat transfer rate is maximum at the bottom left corner and lowest at the right corrugated wall. The fluid is revolving anti-clockwise at a high temperature, which is the physical reason for this phenomenon (higher than hot wall temperature). As a result, the hot wall's left bottom corner created a massive temperature, as depicted in figures. It can be observed from the Fig. 7(a) when Da is small the convection inside the enclosure is strong and the isotherm is considerably distorted. The flat lines of isotherm in the middle of the cavity indicate small conduction. As Da increases, the forced convection is the dominant and circular format of isotherm is created as seen in Fig. 7(d). For the high number of Da, flat lines are negligible due to the greater convection of lid moving. Fig. 7(e)-(h) illustrates the effect on streamlines for various Darcy numbers when it moves towards left and bottom lid walls. One can

15

observe that the domain of the cavity is dominated by two re-circular eddies, which are being created from the moving wall with constant velocity. As Da increases from 10^{-5} to 10 the streamline increases and near the lid wall lines are created in thinner form. Convection is expanded across the fluid rather than localized at the boundary as shown in Fig. 7(h), where the Darcy Number is maximum.

Fig. 8(a) shows the effect of Darcy number on temperature profile at the horizontal mean position of double lid-driven cavity. Because the permeability of the medium increases as the Darcy number rises, the convective mode becomes stronger. As a result, the Darcy number rises, the temperature gradient across the hot wall rises too. For high permeability of the medium more heat is generated near the lid walls. Fig. 8(b) and (c) illustrate that the heat transfer increases with the increase of Darcy number. For higher Da the heat transfer rate is higher in the middle of the cavity and suddenly decreases at 0.9. The external heat increases with increasing or decreasing of internal heat. One can see that the localized clusters with consistent Reynolds number of heat concentrated towards the horizontal boundary, and the cooler parts on the curve boundary. Hence, increased Darcy number causes the convection to increase across the medium as permeability is increased. The symmetric behavior of the bolus can be observed for the high number of Da in the velocity profile in Fig. 8(d) and (e). For smaller Da the horizontal and vertical velocities are the same throughout the region.

4.4 The Absorption/Generation Coefficient

Fig. 9(a)-(e) illustrates the absorption coefficient and Fig. 9(f)-(i) depicts the internal heat generation coefficient effect on isotherms. The heat transfer is significantly increased in the molecular composition of the fluid with increasing internal heat inside the cavity. One can see that for $Q = -1000$ the heat absorption is exceptionally low causing cooler patches within the fluid, however, as the value of Q increases, it is obvious to observe that the internal heat generation is significantly increased within the domain. As increasing the Q we see gradual convection of heat from the vertical boundary into the clockwise spiral motion towards the center of the cross-section. Similarly, in Fig. 9(e)-(f) one can see a more abrupt change in heat flow as the absorption coefficient is increased and heat begins to be generated internally. For the maximum value of Q, the cavity is filled with heat as shown in Fig. 9(i). The heat transfer rate is maximum at the bottom left corner and lowest at the right corrugated wall. The fluid is revolving anti-clockwise at a high temperature, which is the physical reason for this phenomenon (higher than hot wall temperature).

16

As a result, the hot wall's left bottom corner created a massive temperature, as depicted in the Figures.
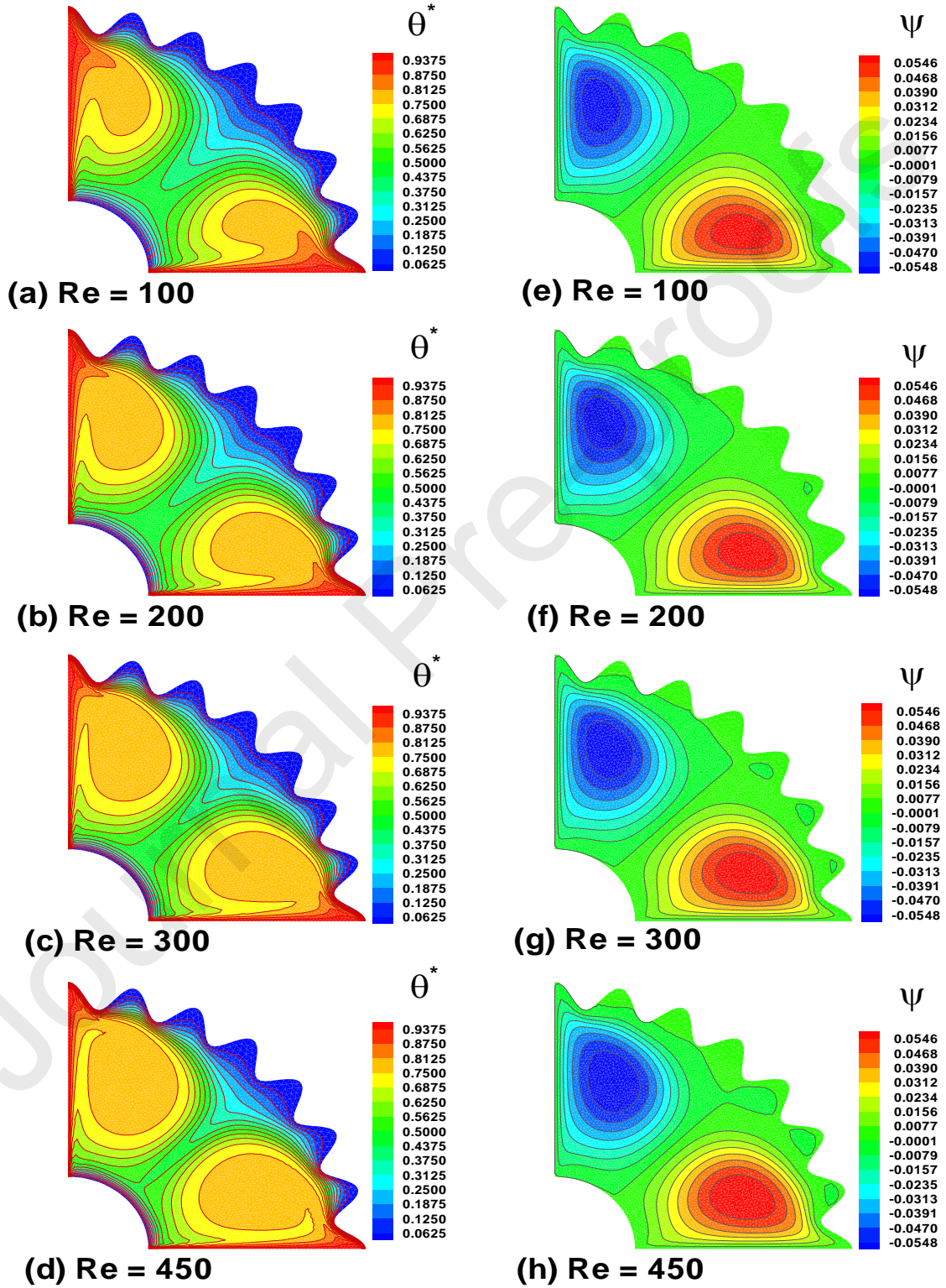

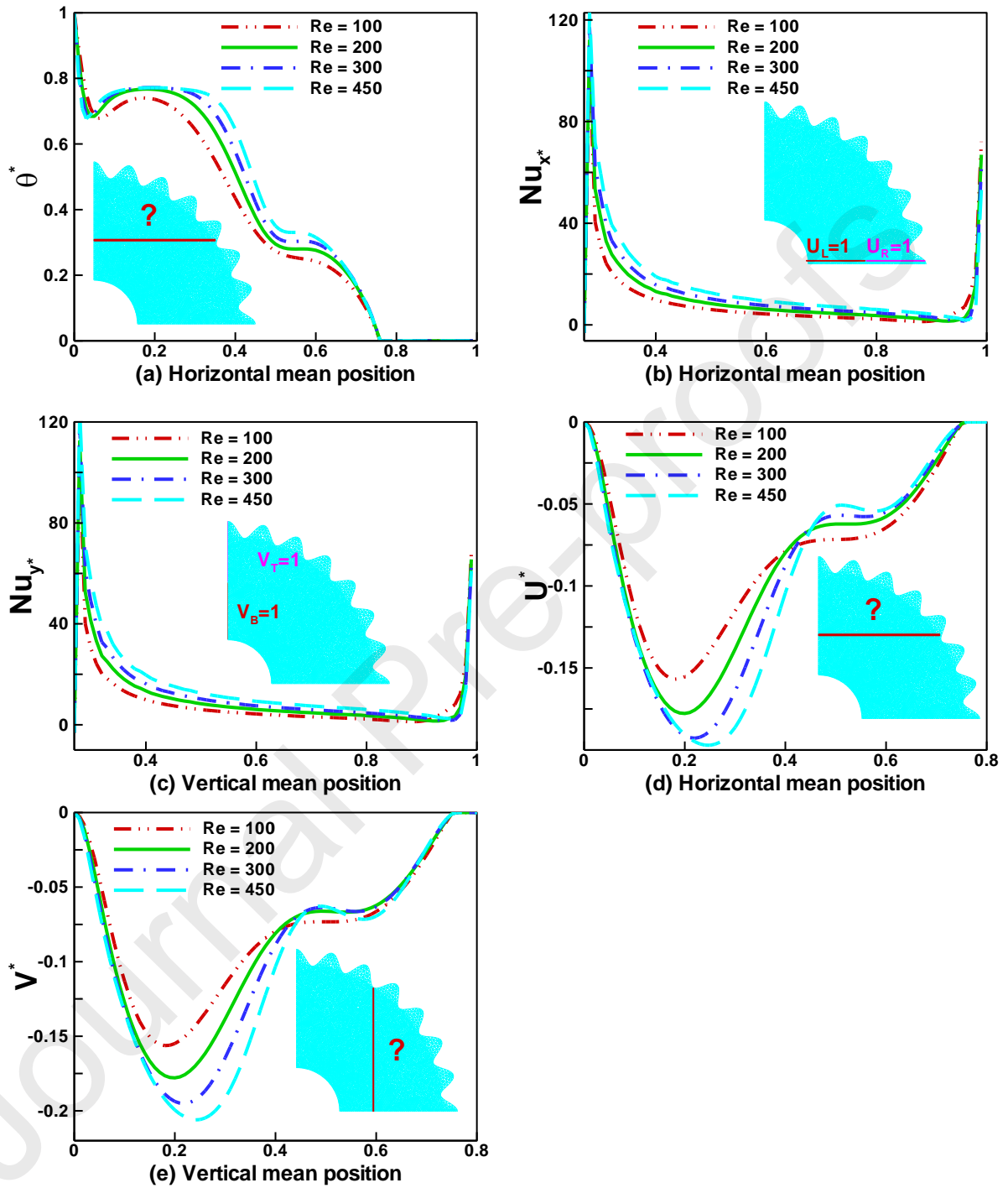**Fig. 5.** Effect of Reynold's number on isotherm (a)-(d) and streamlines (e)-(h)

17

Fig. 6. Effect of various Reynold's number on the Temperature, velocity profile and
Nusselt number

.

(a) Da = 10⁻⁵

(b) Da = 10⁻⁴

(c) Da = 10⁻³

(d) Da = 10

(e) Da = 10⁻⁵

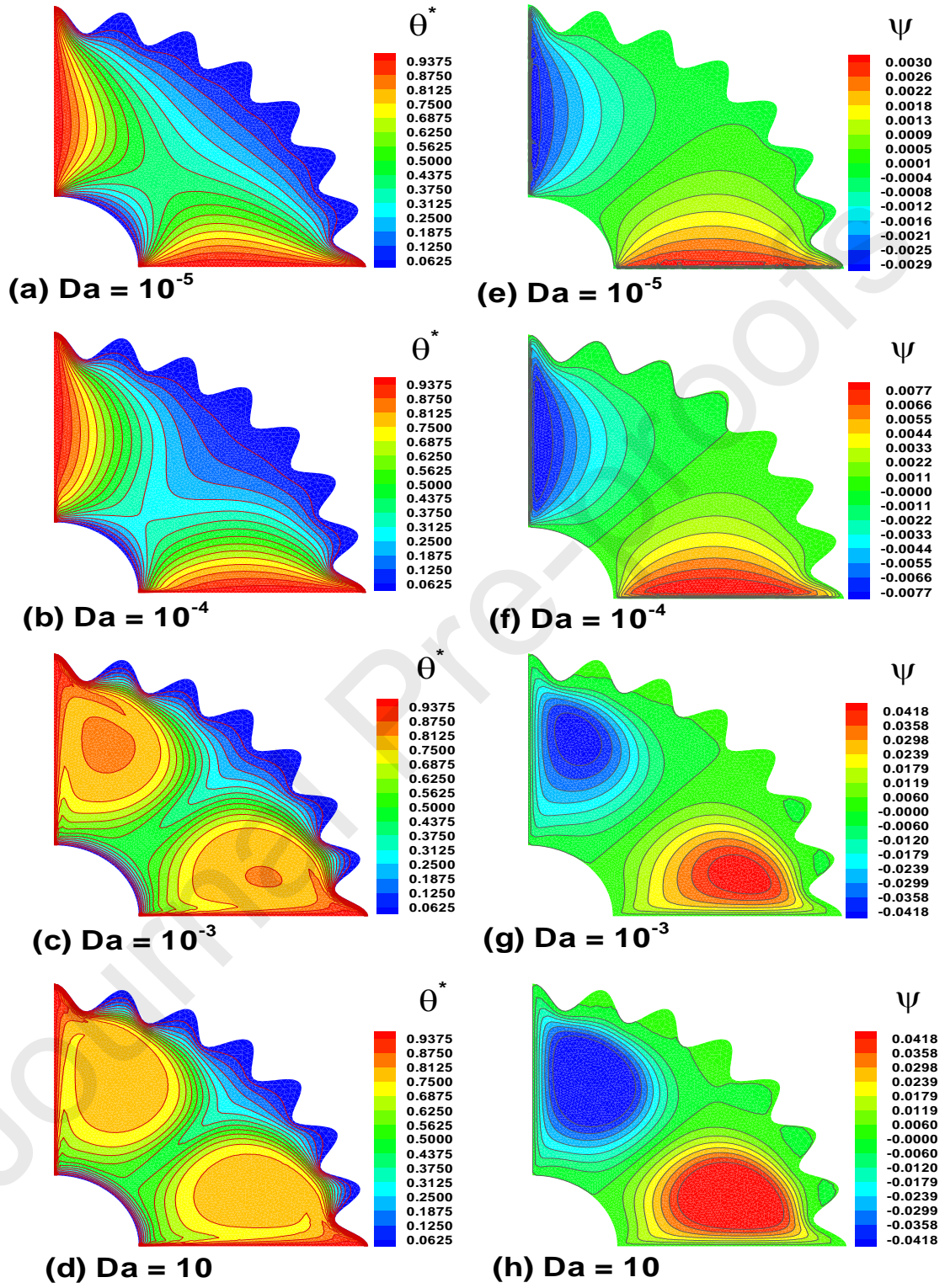**(f) Da = 10⁻⁴**

(g) Da = 10⁻³

(h) Da = 10

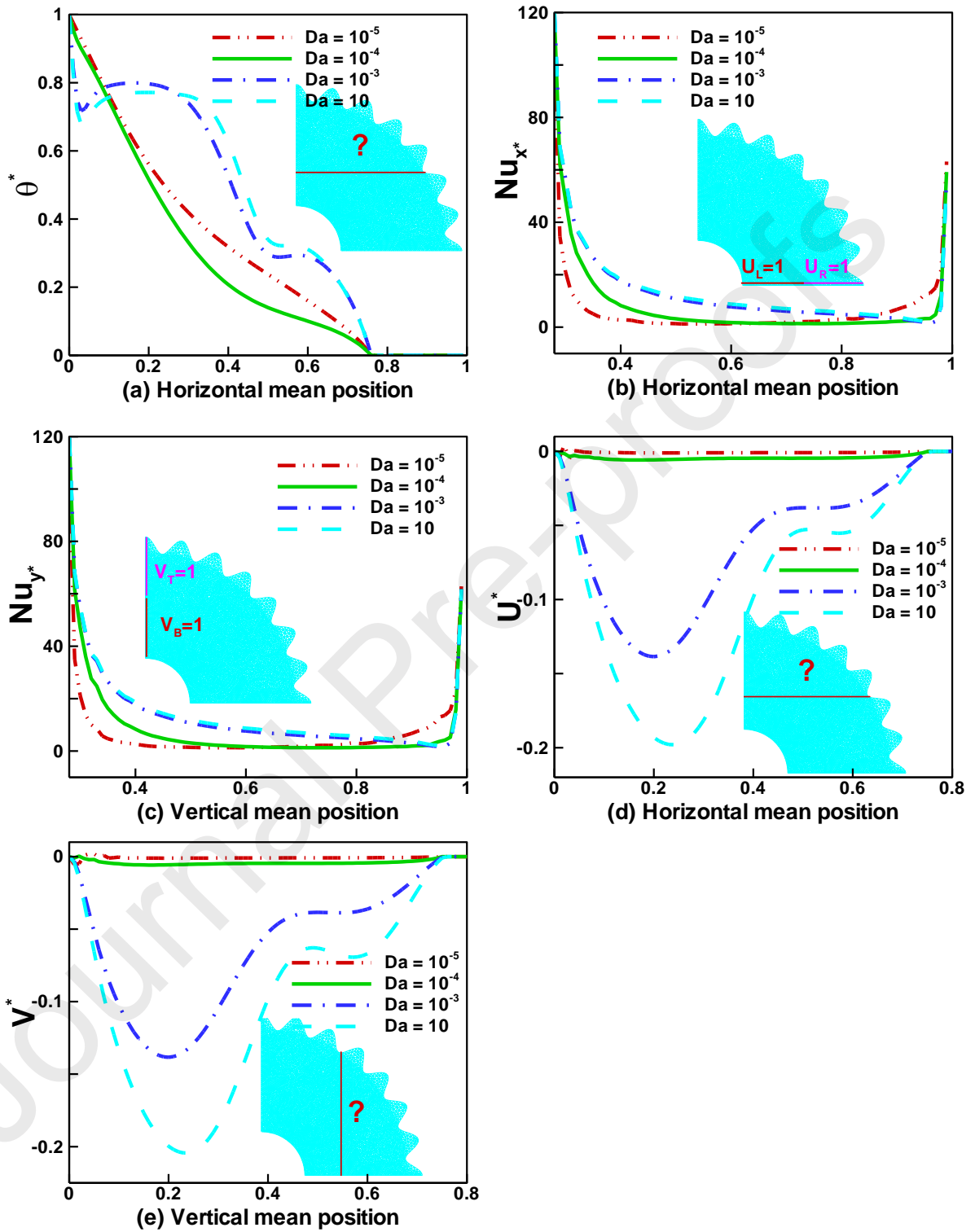**Fig. 7.** Effect of Darcy number on isotherm (a) – (d) and streamlines (e)-(h)

Fig. 8. Effect of various Darcy number on the Temperature, velocity profile and Nusselt number
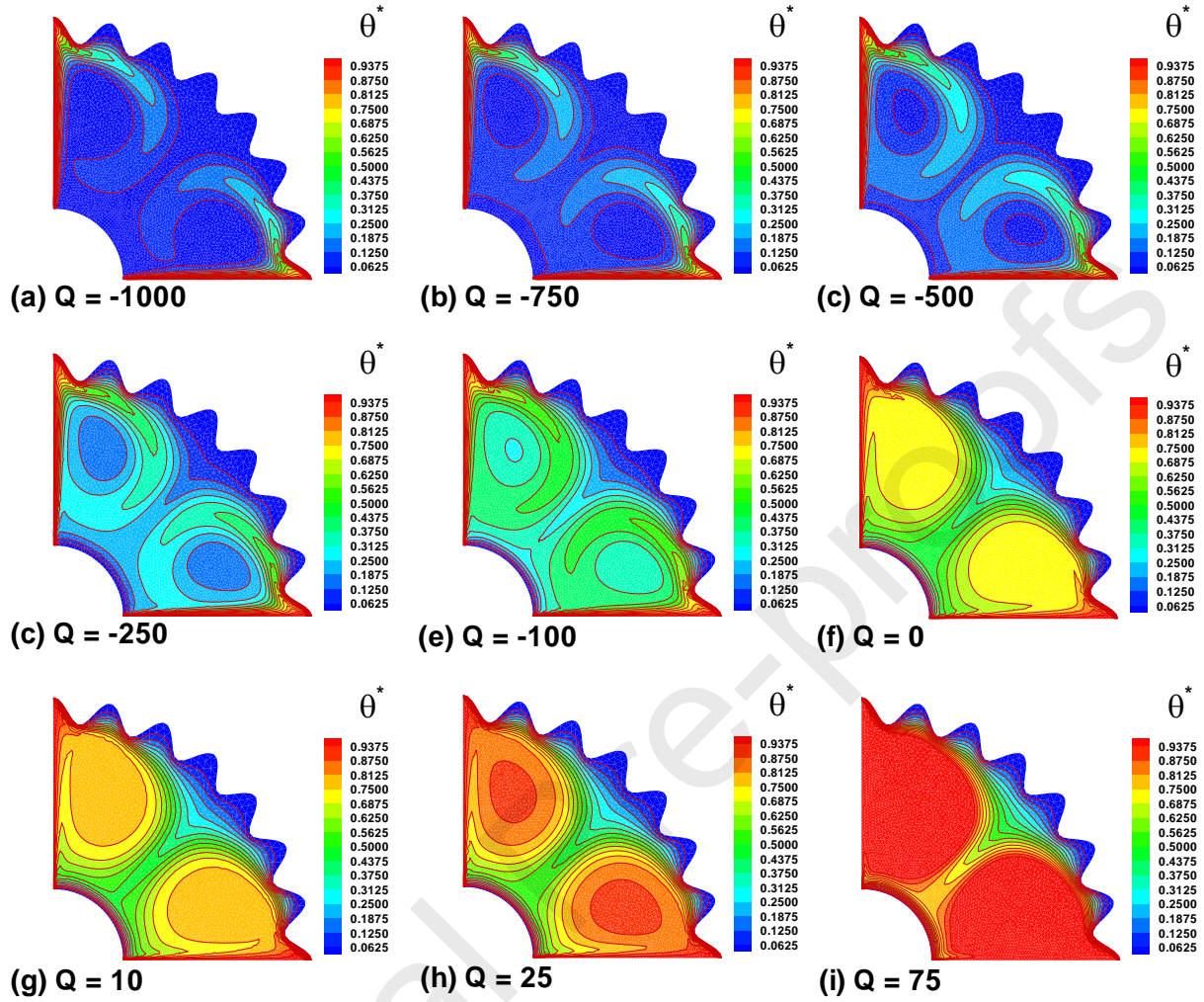
Fig. 9. Effect of Internal heat generation/absorption on isotherm (a) – (i)

Fig. 10(a)-(b) shows the effect of Q at temperature and Nusselt number. The temperature gradient inside the cavity increases with the increase in Q. For a smaller value of Q, internal heat is reduced inside the cavity, which almost approaches zero due to absorption. Heat transfer rate at horizontal mean position decreases with the increasing of Q as shown in Fig. 10(b).

4.5 Effect of concentration of the nanoparticles

The effect of concentration of nanoparticles on isotherm and streamlines are shown in Fig. 11(a)-(c) and 11(d)-(f) respectively. The heat lines decrease with the increase in nanoparticles and the heat transfer is spirally localized near the lid wall. Hence, heat stemming is increased from the vertical and horizontal lid in the case Fig. 11(a) where ϕ=0.0 although this settles as an approach towards Fig. 11(c) where ϕ=0.2, and hence more cooling effect can be seen. From Fig. 11(d) – (f),

21

one can see the streamlines, where the localized hot and cold patches, with the cold regions being vertically dominant, and the greater heat being more dominant at the horizontal boundary
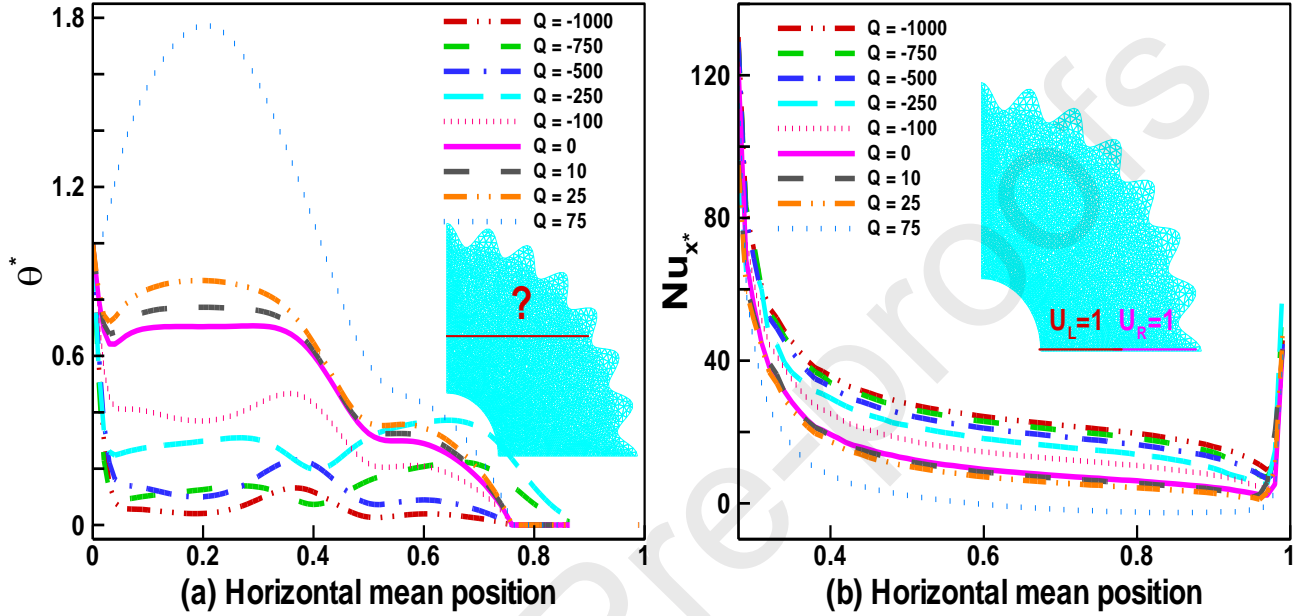

Fig. 10. Effect of internal heat generation/absorption coefficient Temperature profile and Nusselt number

Fig. 12(a)-(f) illustrates the effect of nanoparticles on the Nusselt number, temperature, and both horizontal and vertical velocity profiles. For the base fluid, the maximum temperature is obtained throughout the cavity. But with the increase of nanoparticles, the temperature gradient gradually decreases. Increasing the concentration of solids increases nanofluid thermal conductivity while marginally decreasing the gradient of temperature. Convection in the cavity increases so more heat transfer is done in the cavity that is clearly seen in Fig. 12(b) and (c) in the form of local Nusselt numbers against the horizontal and vertical moving walls. Both horizontal and vertical velocity decrease at the middle of the cavity with increasing concentration of nanoparticles as shown in Fig. 12(d) and (e).

(a) ϕ = 0.0

(b) ϕ = 0.1

(c) ϕ = 0.2

(d) ϕ = 0.0
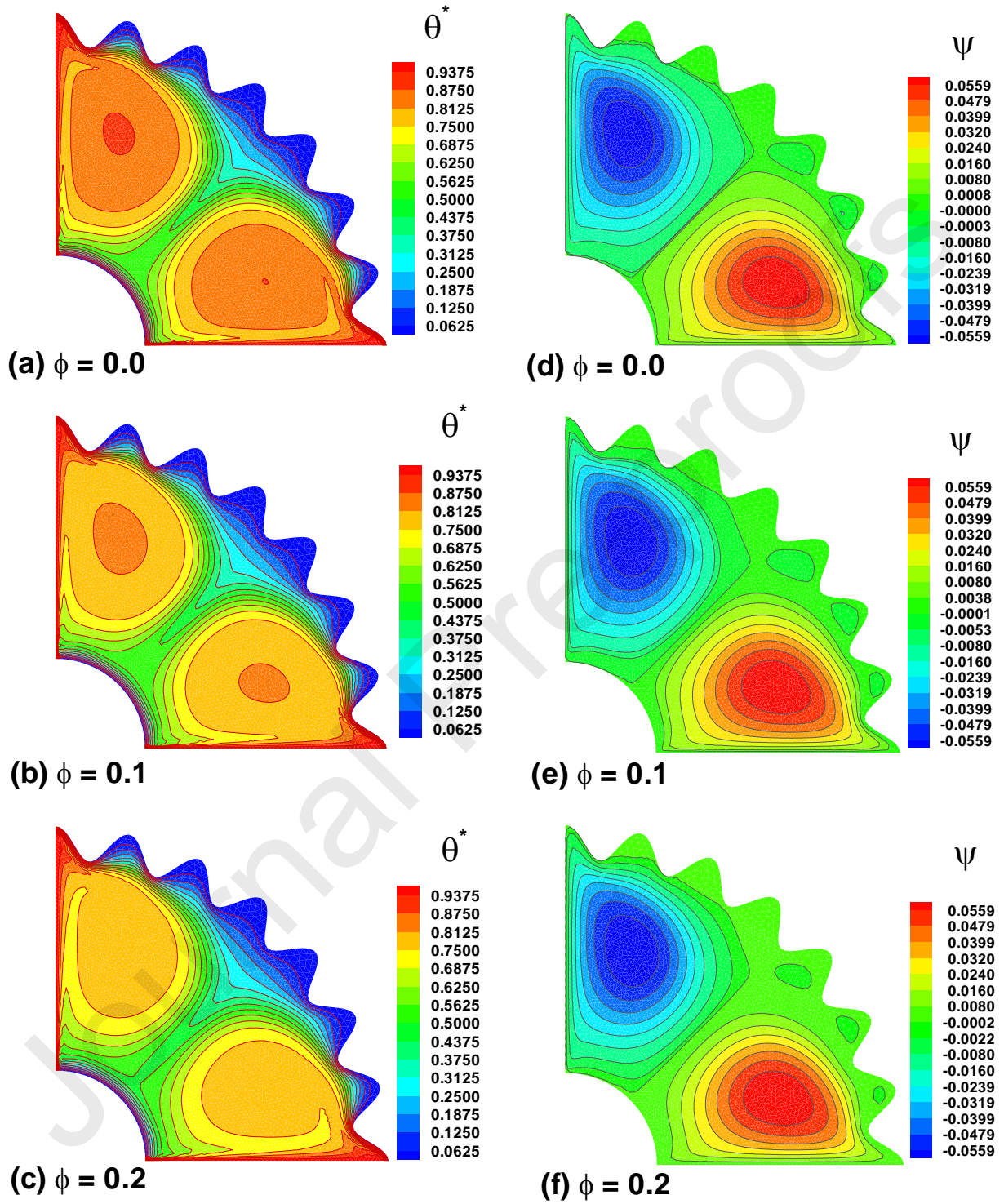
(e) ϕ = 0.1

(f) ϕ = 0.2

Fig. 11. Effect of solid volume fraction of nanoparticles on isotherm (a) – (c) and streamlines (d)-(f)
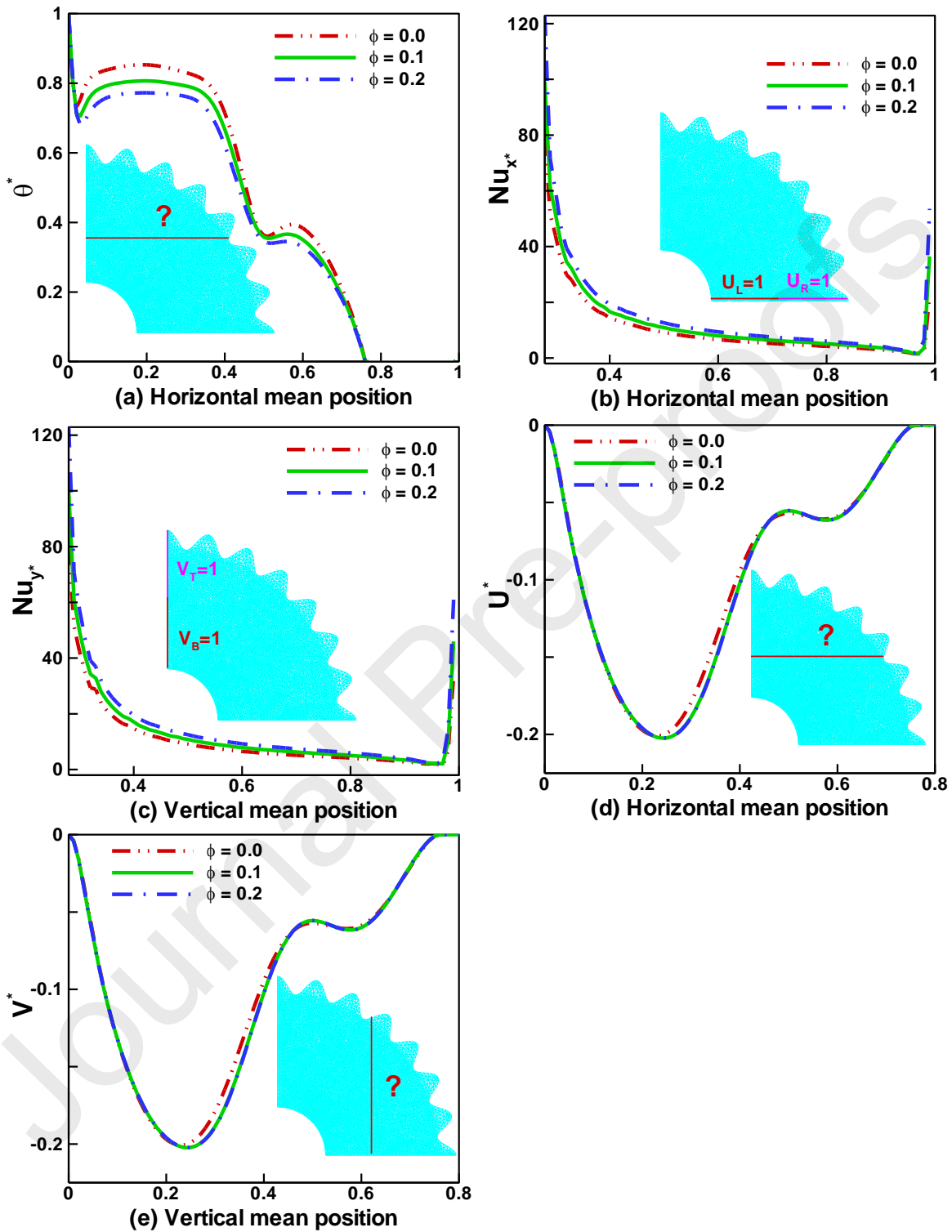
23

Fig. 12. Effect of solid volume fraction of nanoparticles on the Temperature, velocity profile, and Nusselt number

24

5. Conclusions

After carefully examining the present model, we have developed the conclusion that describes the key factor of the entire study. As defined in the model, the current model is based upon forced convection due to lid-driven of left vertical and bottom horizontal walls. We have discussed the different directions of moving lid, then we analyze the model for the various value of Reynolds number, Richardson number, heat generation parameter, porous medium, and nanoparticle volume fraction. All the effects are discussed for velocity, temperature, stream function, and isotherms. Following are the key findings of the present model.

- In isotherms, the opposing directional (inside) movement of the lid walls generates more heat inside the cavity.

- In streamlines, the opposite directions of velocity produce more eddies than the velocity in the same direction.

- The effect of velocity (in opposite outward direction) yields the maximum flow of heat transfer at the mean position from where it acts like a symmetric behavior in the local Nusselt number.

- An increase in Reynolds number has caused an increase in isotherm lines and this effect on streamline causes the eddies movement towards the center.

- Maximum velocity is observed in both ends of the cavity and minimum in the middle with a greater Reynolds number.

- An increase in permeability region decreases the heat generation near the lid walls and pushes them away from the lid wall.

- Increasing permeability decreases the local Nusselt number.

- For the minimum value of Q, heat is absorbed in the cavity and restricted to the lid walls whereas there is a maximum heat generator in the cavity for a greater value of $Q = 75$.

- Local Nusselt number decreases with an increase in heat absorption coefficient.

- Temperature profile decreases with an increase in nanoparticles while Nusselt number increases with increasing ϕ.

Author's contribution:

Anh Tuan Hoang: Conceptualization; review & editing; **Rizwan Ul Haq**: Project administration, Supervision, Writing - review & editing; **Syed Saqib Shah**: Supervision, Writing - review &

editing; **Tri Hieu Le**: Supervision, Review & editing; **Luthais B. McCash**: Review & editing.

6. References

[1]. N. Putra et al., "Natural Convection of Nanofluids", *Int. J. Heat Mass Transf.* 39 (2003) 8 775-784.

[2]. W. Daungthongsuk, S. Wongwises, "A Critical Review of Convective Heat Transfer Nanofluids", *Renewable & Sustainable Energy Reviews*: 11 (2007) 797-817.

[3]. V. Trisaksri, S. Wongwises, "Critical Review of Heat Transfer Characteristics of Nanofluids", *Renewable & Sustainable Energy Reviews*: 11 (2007) 512-523.

[4]. S. Kakac, A. Pramuanjaroenkij, "Review of Convective Heat Transfer Enhancement with Nanofluids", *Int. J. Heat Mass Transf.* 52 (2009) 3187-3196.

[5]. R. Saidur et al., "A Review on Applications and Challenges of Nanofluids", *Renewable & Sustainable Energy Reviews*: 15 (2011) 1646-1668.

[6]. R. U. Haq, S. N. Kazmi, T. Mekkaoui, "Thermal management of water based SWCNTs enclosed in a partially heated trapezoidal cavity via FEM", *Int. J. Heat Mass Transf.* 112 (2017) 972–982.

[7]. M. A. Mansour, S. E. Ahmed, "Mixed convection flows in a square lid driven cavity with heat source at the bottom utilising nanofluid" *Can. J. Chem. Eng.* 90, 100 (2012).

[8]. A. Boutra, K. Ragui, Y. K. Benkahla, "Numerical study of mixed convection heat transfer in a lid-driven cavity filled with a nanofluid," *Mech. Ind.* 16, 505 (2015).

[9]. M. H. Esfe, M. Akbari, and A. J. Karimipour, "Mixed convection in a lid-driven cavity with an inside hot obstacle filled by an Al_2O_3–water nanofluid" *J. Appl. Mech. Tech. Phys.* 56 (2015) 443.

[10]. A. A. A. Arani, S. Mazrouei Sebdani, M. Mahmoodi, A. Ardeshiri, M. Aliakbari, "Numerical study of mixed convection flow in a lid-driven cavity with sinusoidal heating on sidewalls using nanofluid" *Superlattices Micro-struct*. 51, 893 (2012).

[11]. A. Ghofrani, M.H. Dibaei, A. Hakim Sima, M.B. Shafii, "Experimental investigation on laminar forced convection heat transfer of ferrofluids under an alternating magnetic field", *Exp. Thermal Fluid Sci*. 49 (2013) 193–200.

[12]. R. Nasrin, et al., Combined Convection Flow in Triangular Wavy Chamber Filled with Water-CuO Nanofluid: Effect of Viscosity Models, *Int. Comm. Heat Mass Transf*. 39 (2012) 1226-1236.

[13]. B. C. Pak, Y. Cho, "Hydrodynamic and Heat Transfer Study of Dispersed Fluids with Submicron Metallic Oxide Particle", *Experimental Heat Transfer*: 11 (1998) 151-170.

[14]. H. C. Brinkman, "The Viscosity of Concentrated Suspensions and Solutions", *Journal of Chemical Physics*: 20 (1952) 571-581.

[15]. C. J. Ho, M. W. Chen, Z. W. Li, "Numerical simulation of natural convection of nanofluid in a square enclosure: effects due to uncertainties of viscosity and thermal conductivity", *Int. J. Heat Mass Transf.* 51 (2008) 4506–4516.

[16]. M. Izadi, A. Behzadmehr, D. Jalali-Vahida, "Numerical study of developing laminar forced convection of a nanofluid in an annulus", *Int. J. Therm. Sci.* 48 (2009) 2119–2129.

[17]. M. Mahmoodi, "Mixed convection inside nanofluid filled rectangular enclosures with moving bottom wall" *Thermal Sci.* 15 (2011) 889–903.

[18]. M. Sebdani, M. Mahmoodi, S. M. Hashemi, "Effect of nanofluid variable properties on mixed convection in a square cavity" *Int. J. Thermal Sci.* 52 (2021) 112–126.

[19]. R. A. Mahdi, H. A. Mohammed, K. M. Munisamy, N. H. Saeid, "Review of convection heat transfer and fluid flow in porous media with nanofluid" *Renewable & Sustainable Energy Reviews.* 41 (2015) 715–734.

[20]. G. C. Bourantas, E. D. Skouras, V. C. Loukopoulos, V. N. Burganos, "Heat transfer and natural convection of nanofluids in porous media" *Eur. J. Mech. B, Fluids* 43 (2014) 45–56.

[21]. M. Zhang, W. Qiuwei, J. Wen, Z. Lin, F. Fang, Q. Chen, "Optimal operation of integrated electricity and heat system: A review of modeling and solution methods" *Renewable & Sustainable Energy Reviews* 135 (2021) 110098.

[22]. F. Ran, Y. Chen, R. Cong, G. Fang, "Flow and heat transfer characteristics of microencapsulated phase change slurry in thermal energy systems: A review", *Renewable & Sustainable Energy Reviews* 134 (2020) 110101.

[23]. M. Tahmasbi, M. Siavashi, H. Z. Abbasi, M. Akhlaghi, "Mixed convection enhancement by using optimized porous media and nanofluid in a cavity with two rotating cylinders" *Journal of Thermal Analysis and Calorimtry* 141 (2020) 1829-1846.

[24].   P. Geridonmez, H. F. Ozotop, "Natural convection in a cavity filled with porous medium under the effect of a partial magnetic field" *Int. Journal of Mechanical Sciences* 161–162 (2019) 105077.

[25].   M. Tahmasbi, M. Siavashi, A. M. Norouzi, M. H. Doranehgard, "Thermal and electrical efficiencies enhancement of a solar photovoltaic-thermal/air system (PVT/air) using metal foams" *Journal of the Taiwan Institute of Chemical Engineers* 124 (2021) 276-289.

[26].   N. A. Libdeh, F. Redouane, A. Aissa, F. M. Oudina, A. Almuhtady, W. Jamshed, W. Al-Kouz, "Hydrothermal and Entropy Investigation of $Ag/MgO/H_2O$ Hybrid Nanofluid Natural Convection in a Novel Shape of Porous Cavity" *Appl. Sci.* 11 (2021) 1722 https://doi.org/10.3390/app11041722.

[27].   Q. Xiong, M. Siavashi, M. H. Doranehgard, M. M. Nezhad, "Recant development of advanced numerical heat transfer in porous media" *Journal of Thermal Analysis and Calorimtry* 141 (2020) 1489-1491.

[28].   S. Nazari, R. Ellahi, M. M. Sarafraz, M. R. Safaei, A. Asgari, O. A. Akbar, "Numerical study on mixed convection of a non-Newtonian nanofluid with porous media in a two lid-driven square cavity" *Journal of Thermal Analysis and Calorimtry* 140 (2020) 1121-1145.

[29].   M. H. Toosi, M. Siavashi, "Two-phase mixture numerical simulation of natural convection of nanofluid flow in a cavity partially filled with porous media to enhance heat transfer" *Journal of Molecular Liquid* 238 (2017) 553-569.

[30].   A. Bairi, "Using nanofluid saturated porous media to enhance free convective heat transfer around a spherical electronic device" *Chinese Journal of Physics* 70 (2021) 106-116.

[31].   D. Chatterjee, S.K. Gupta, B. Mondal, "Mixed convective transport in a lid-driven cavity containing a nanofluids and a rotating circular cylinder at the center" *Int. Comm. Heat Mass Transf.* 56 (2014) 71–78.

[32].   M. N. A. W. M. Yazid, N. A. C. Sidika, W. J. Yahya, "Heat and mass transfer characteristics of carbon nanotube nanofluids A review" *Renewable & Sustainable Energy Reviews* 80 (2017) 914–941.

[33].   A. I. Alsabery, I. Hashim, A. J. Chamkha, H. Saleh, B. Chanane, "Effect of spatial side-wall temperature variation on transient natural convection of a nanofluid in a trapezoidal cavity" *Int. J. Numer. Methods Heat Fluid Flow* 27 (2017) 1365–1384.

[34]. A. J. Chamkha, "Hydromagnetic combined convection flow in a vertical lid-driven cavity with internal heat generation or absorption" *Numer. Heat Transf.* 41 (2002) 529-546.

[35]. H. F. Oztop, K. Al-Salem, I. Pop, "MHD mixed convection in a lid-driven cavity with corner heater" *Int. J. Heat Mass Transf.* 54 "2011" 3494–3504.

[36]. M. A. Sheremet, I. Pop, R. Nazar, "Natural convection in a square cavity filled with a porous medium saturated with a nanofluid using the thermal non-equilibrium model with a Tiwari and Das nanofluid model" *Int. J. Mech. Sci.* 100 (2015) 312–321.

[37]. M. Sheikholeslami, M. Shamlooei, "Magnetic source influence on nanofluid flow in porous medium considering shape factor effect" *Phys. Lett. A* 381 (2017) 3071–3078.

[38]. M. Sheikholeslami, Li. Zhixiong, M. Shamlooei, "Nanofluid MHD natural convection through a porous complex shaped cavity considering thermal radiation" *Phys. Lett. A* 382 (24) (2018) 1615–1632.

[39]. R. U. Haq, I. Rashid, Z. H. Khan, "Effects of aligned magnetic field and CNTs in two different base fluids over a moving slip surface" *J. Mol. Liq.* 243 (2017) 682–688.

[40]. N. Shahzad, A. Zeeshan, R. Ellahi, K. Vafai, "Convective heat transfer of nanofluid in a wavy channel: Buongiorno's mathematical model" *J. Mol. Liq.* 222 (2016) 446–455.

[41]. A. F. Khudheyer, "MHD mixed convection in double lid-driven differentially heated trapezoidal cavity" *Int. J. Appl. Innovat. Eng. Manage.* 4 (2015).

[42]. S. Sivasankaran, V. Sivakumar, A. K. Hussein, "Numerical study on mixed convection in an inclined lid-driven cavity with discrete heating" *Int. Comm. Heat Mass Transfer* 46 (2013) 112–125.

[43]. A. S. Dogonchi, A. J. Chamkha, M. A. Ismael, D. D. Ganji, "Numerical analysis of natural convection of Cu- water nanofluid filling triangular cavity with semi-circular bottom wall" *Journal of Thermal Analysis and Calorimetry* 135 (2019) 3485–3497.

[44]. A. I. Alsabery, M. A. Ismael, A. J. Chamkha, I. Hashim, "Effect of two-phase nanofluid model on MHD mixed convection in a lid-driven cavity in the presence of conductive inner block and corner heater" *Journal of Thermal Analysis and Calorimetry* 135 (2019)729–750.

[45]. A. I. Alsabery, M. A. Ismael, A. J. Chamkha, I. Hashim, "Mixed convection of Al_2O_3-water nanofluid in a double lid-driven square cavity with solid inner insert using Buongiorno's two-phase model" *Int. J. Heat Mass Transf.* 119 (2018) 939-961.

[46]. M. A. Ismael, Double- diffusive mixed convection in a composite porous enclosure with arc- shaped moving wall: Tortuosity effect, J. Porous Media 21 (2018) 343-362.

[47]. M. A. Ismael, M. A. Mansour, A. J. Chamkha, A. M. Rashad, "Mixed convection in a nanofluid filled-cavity with partial slip subjected to constant heat flux and inclined magnetic field" *J. Magnetism & Magnetic Materials* 416 (2016) 25-36.

[48]. Anh Tuan Hoang, Waste heat recovery from diesel engines based on Organic Rankine Cycle, Applied Energy, 231 (2018) 138-166.

[49]. Anh Tuan Hoang, Xuan Phuong Nguyen, Anh Tuan Le, Minh Tuan Pham, Trung Huan Hoang, Abdel Rahman M. Said Al-Tawaha, Surfa Yondri, Power generation characteristics of a thermoelectric modules-based power generator assisted by fishbone-shaped fins: Part II – Effects of cooling water parameters, Energy Sources, Part A: Recovery, Utilization, and Environmental Effects 43(3) (2021) 381-393.

[50]. Tri Hieu Le, Minh Tuan Pham, H Hadiyanto, Van Viet Pham, Anh Tuan Hoang, Influence of Various Basin Types on Performance of Passive Solar Still: A Review, International Journal of Renewable Energy Development, 10(4) (2021) 789-802.

[51]. A. Chattopadhyay, S. K. Pandit, S. S. Sarma, I. Pop, "Mixed convection in a lid-driven sinusoidally heated porous cavity" *Int. Journal of Heat and Mass Transf.* 93 (2016) 361-378.

[52]. J. Maxwell, "A Treatise on Electricity and Magnetism" *Oxford University Press, Cambridge* UK, 1904.

[53]. O. C. Zienkiewicz, R. L. Taylor, P. Nithiarasu "The finite element method for fluid dynamics" *Amsterdam 6th edn. Elsevier* (2005).

[54]. R. Codina, "Comparison of some finite element methods for solving the diffusion-convection-reaction equation" *Comput Methods Appl Mech Eng* 156(1–4) (1998) 185–210.

[55]. K. M. Khanafer, A. J. Chamkha, "Mixed convection flow in a lid driven enclosure filled with a fluid saturated porous medium" *Int. J. Heat Mass Transf.* 31 (1999) 2465-2481.

[56]. R. Iwatsu, J. M. Hyun, K. Kuwahara, "Mixed convection in a driven cavity with a stable vertical temperature gradient" *Int. J. Heat Mass Transf.* 36 (1993) 1601-1608.